COLD CRUCIBLE MELTING WITH BOTTOM POURING NOZZLE

Journal:	*COMPEL: The International Journal for Computation and Mathematics in Electrical and Electronic Engineering*
Manuscript ID	COMPEL-05-2019-0208.R1
Manuscript Type:	Original Article
Keywords:	Induction heating, Magnetic levitation, Magnetohydrodynamics, Time-domain modelling

COLD CRUCIBLE MELTING WITH BOTTOM POURING NOZZLE

ABSTRACT. Cold crucible melting technique with electromagnetic induction is used to obtain reactive metal castings and produce high quality metal powders for aerospace, automotive and medical applications. An important part of this technology is the nozzle used to pour the molten alloy through the bottom opening. The paper uses mathematical modelling technique, previously validated on multiple similar cases, to investigate a new type of non-consumable nozzle made of copper segments. The design of the nozzle requires to satisfy the narrow balance between the thin solidified protective layer on the wall while avoiding the blockage of the outflow if the nozzle is frozen completely. The sensitivity of the outflow to the nozzle diameter is investigated. The AC electromagnetic force leads to high mixing rates, transitional flow structures and turbulence of the melt, contributing to the melt shape dynamics and the heat loss to walls. The beneficial features of the cold crucible melting to purify the melt from particulate contamination are explained using the particle tracking for the full melting and pouring cycle.

INTRODUCTION

Titanium alloys are increasingly used in aerospace and automotive applications. New melting techniques and practices are required to achieve desirable mechanical properties for critical components [1]. The cold crucible technique, alternatively known as the induction skull melting (ISM), is commonly used to melt the titanium alloys with additional stirring created by electromagnetic forces. The intense stirring is essential in preparing homogeneous alloys when adding uniformly dispersed grain refiners or micro to nano size particles to create a composite alloy of enhanced mechanical properties [2]. At the same time refinement of the alloy from larger oxide particles and film fragments of macro size (100 micron and larger) is highly desirable. The ISM technique is proven to be most effective to obtain reactive metal castings and produce high quality metal powders. A critical step in casting these components is the way how the prepared liquid alloy is delivered to the casting mold. Using the tilt casting technique the liquid alloy experiences significant loss of the required superheat [6], therefore various bottom pouring techniques were proposed. The graphite/ceramics nozzle [1] is the most successful in industrial applications, however suffers from deterioration due to erosion and needs replacement after each casting. A new type of nozzle composed of copper segments was tried and tested in [4,5], however the design did not find a widespread application due to uncontrollable outflow from the crucible and the low energy efficiency. Therefore a new type of copper nozzle is proposed in this paper. This nozzle is intended to replace the existing ceramics nozzle by a suitable size copper nozzle composed of water cooled segments. To design this nozzle a careful selection of the operating parameters is required accounting for the solidifying skull formation and the melt outflow to the nozzle.

There is a variety of mathematical modelling attempts of the ISM to mention just the few representative publications [3-8] and the references therein. The present paper presents the fully dynamic simulation of the melting including the dynamic free surface resolution during the full bottom pouring cycle of the cold crucible operation. This is achieved using the previously validated spectral code SPHINX [6-9]. The code is supplemented by the Lagrangian particle tracking module in attempts to give insight to the behavior of various inclusions and possible

separation in the ISM process [7,8]. The paper demonstrates the importance of the AC magnetic interaction effects on the particle transport and the eventual separation during the cold crucible operation accounting for the solidifying skull formation and the melt outflow to the nozzle at the bottom. The non-consumable nozzle made of copper segments could help to solve the problem of the short life cycle of traditional graphite/ceramics type of nozzles used in the existing ISM devices [1].

NUMERICAL MODEL DESCRIPTION

The equations solved by the numerical model are the momentum and mass conservation equations for the incompressible fluid with the effective viscosity ν_e and the turbulent diffusivity α_e modified heat transfer equations:

$$\partial_t \mathbf{v} + (\mathbf{v}\cdot\nabla)\mathbf{v} = -\rho^{-1}\nabla p + \nabla\cdot(\nu_e(\nabla\mathbf{v} + \nabla\mathbf{v}^T)) + \rho^{-1}\mathbf{f}_{AC} + \mathbf{g}\,, \tag{1}$$

$$\nabla\cdot\mathbf{v} = 0\,, \tag{2}$$

$$C_p^*(\partial_t T + \mathbf{v}\cdot\nabla T) = \nabla\cdot(C_p\alpha_e\nabla T) + \rho^{-1}\,|\,\mathbf{J}\,|^2/\sigma\,, \tag{3}$$

The usual notation is used, given in detail elsewhere [7]. The full boundary conditions for the velocity include the no-slip condition at the solid container walls

$$\mathbf{v} = 0\,, \tag{4}$$

at the free surface the normal stress is determined by the pressure p_a in the space above the crucible and the surface tension:

$$\mathbf{e_n}\cdot\Pi\cdot\mathbf{e_n} = p_a + \Gamma K\,. \tag{5}$$

The pressure p_b is prescribed at the nozzle exit. On the liquid metal free surface the continuity of the velocity field and the tangential stress conditions are required:

$$\nabla\cdot\mathbf{v} = 0\,,\quad \mathbf{e_n}\cdot\Pi\cdot\mathbf{e}_\tau = 0\,, \tag{6}$$

where $\boldsymbol{e}_n, \boldsymbol{e}_\tau$ are the unit vectors normal and tangential to the free surface, Π is the stress tensor, K is the surface curvature. The free surface shape **R**(t) is updated at each time step using the kinematic condition:

$$\partial_t\mathbf{R}\cdot\mathbf{e_n} = \mathbf{v}\cdot\mathbf{e_n} \tag{7}$$

The previously validated [6] 'k-ω' turbulence model including the effect of magnetic damping is used to calculate the effective viscosity ν_e and the turbulent diffusivity α_e. The thermal boundary conditions account for the radiation losses, the high vapour pressure alloy component evaporation, and the heat loss to the water-cooled solid surface of the crucible and the nozzle [6].

In the pseudo-spectral code SPHINX the electromagnetic force is computed from an integral equation representation. This has an advantage that the boundary conditions are not explicitly required and the electromagnetic field can be solved only in the regions where it is needed. The electric current distribution in a moving medium of conductivity σ is then given by the magnetic

vector potential **A**, the magnetic field $\mathbf{B} = \nabla \times \mathbf{A}$, the electric potential φ and the fluid flow induced part $\sigma \mathbf{v} \times \mathbf{B}$:

$$\mathbf{j} = \sigma(-\partial_t \mathbf{A} - \nabla\varphi + \mathbf{v} \times \mathbf{B}) = \mathbf{j}_{AC} + \mathbf{j}_{\mathrm{v}}. \quad (8)$$

The $\mathbf{j}_{AC}$ part of the current is induced in the conducting medium even in the absence of velocity. The governing integral equations can be obtained from the electric current distribution in the source coils and the unknown induced currents in the liquid related to the total magnetic field and the vector potential **A** by the Biot-Savart law:

$$\mathbf{A}(\mathbf{r}) = \tfrac{1}{4\pi} \int \mathbf{j}(\mathbf{r}')/ \,|\, \mathbf{r} - \mathbf{r}' \,|\, \mathrm{d}\,\mathbf{r}' \quad (9)$$

The equations (8) and (9) can be solved efficiently in the axisymmetric case for harmonic fields. The induced current in the liquid drop depends on its instantaneous free surface shape and needs to be recomputed as the shape changes during the oscillation development. The resulting electromagnetic force **f**, time-averaged over the AC period, similarly to (8) can be decomposed in two parts: $\mathbf{f} = \mathbf{f}_{AC} + \mathbf{f}_{\mathrm{v}}$. The second, fluid velocity dependent part of the force $\mathbf{f}_{\mathrm{v}}$ can include DC and AC time-averaged contributions. In the presence of AC fields originating from different sources, as in the ISM containing the main coil at the side of the crucible and the bottom coil at the nozzle, the superposition of the time average force contributions and the Joule heating in the liquid metal are used.

The equations (1)-(9) are solved by the spectral collocation method with the Chebyshev grid for the radial direction and Legendre nodes in the vertical direction. The numerical solution method is based on the continuous co-ordinate transformation adapting to the free surface and the containing vessel shape at the consecutive time steps. The stable time integration of the solution is based on adjustable time steps of the order 0.1 – 2 ms for the unsteady fluid flow solution in the examples considered below.

EXAMPLES OF SIMULATION RESULTS

The mathematical modelling of the complex time dependent problem starts initially with heating a cylindrical TiAl solid of 50 kg weight, leading to the gradual melting process and subsequent liquid metal magnetic confinement dynamics, turbulent fluid flow and the temperature evolution. In the present ISM setup two different coils are used: one at the side (lower frequency ~ 5 kHz) and the second smaller at the nozzle (~50 kHz). The time dependent Joule heating eventually leads to melting of the solid ingot. When the solidus temperature is reached, the model accounts for the phase transition and the following liquid material shape change due to the action of the EM force distribution adjusted to the moving solid/liquid and the free interface. The electromagnetic field induces a strong turbulent flow in the molten pool, which is beneficial for producing a homogeneous melt with uniform temperature. The process combines induction melting and pouring via the bottom nozzle into a single self-controlling operation.

After the initial melting stage practically all volume of the titanium aluminide alloy is in liquid phase shaped as typical dome (Figure 1a). The action of the bottom coil at all following stages (Figure 1) helps to maintain the nozzle free from solid phase, except from the extremely thin solidified skull acting as a protecting film between the out flowing liquid metal and the copper segmented wall of the nozzle. The side skull thickness gradually grows, particularly in the bottom part, until the accelerated solidification starts at the end stages of the pouring (Figure 1d) due to the fast decrease of inductive coupling to the melt and decrease in the Joule heating delivered to the melt (Figure 2).

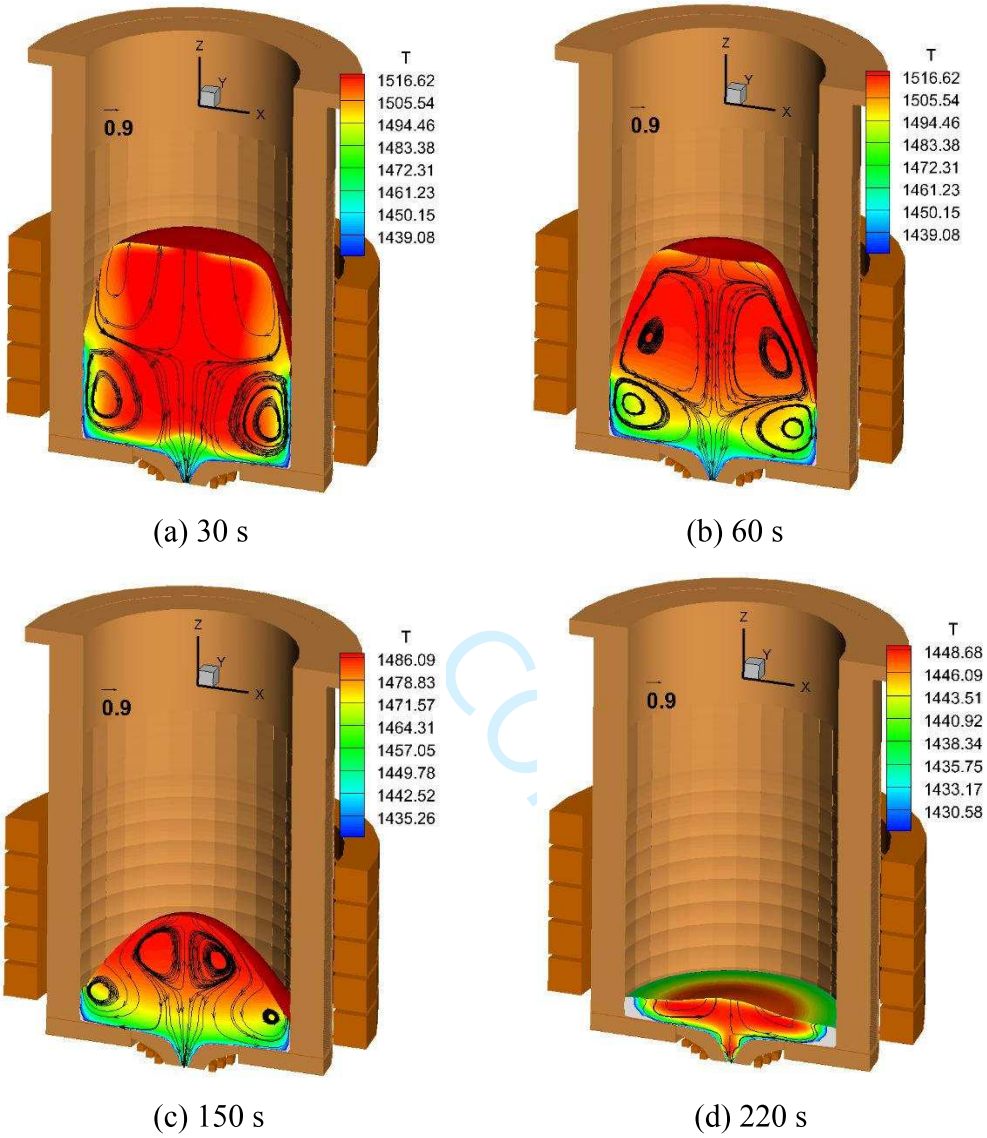

Figure 1. Dynamic stages of the cold crucible operation with the nozzle d = 8 mm: a) the initial stage after complete melting is achieved, b) the following stage when pouring starts, the volume decreases and the dome shape is stabilised, c) the late stage of pouring when the power coupling is reduced, d) the final stage just before the end of pouring.

The action of the EM force in the nozzle region affects the outflow rate which is monitored during the full simulation cycle. Figure 3 shows the predicted outflow rate and the moderate superheat of about 20 degrees C, which is fluctuating due to the turbulent flow and the free metal surface oscillation. The average temperature drops with the decrease in the Joule heating delivered to the melt with the decrease of electromagnetic coupling between the liquid metal volume and the copper crucible segments. The outflow temperature depends significantly on the nozzle diameter as shown in the Figure 3. The outflow rate and its stability can be controlled additionally by adjusting the current magnitude and the AC frequency of the nozzle surrounding coil. This is particularly important if a slow rate of outflow at a higher superheat is desired. When the extremely narrow nozzle of 4 mm diameter is needed, this requires a careful

adjustment of the current and frequency to prevent an unstable outflow. Figure 4 shows the final stage of the crucible operation when the bottom skull grows fast and the nozzle eventually freezes over. Even at this stage it is possible to remelt the frozen nozzle exit if increasing the current in the bottom coil, however the heat removal in the bottom copper segments need to be strictly controlled.

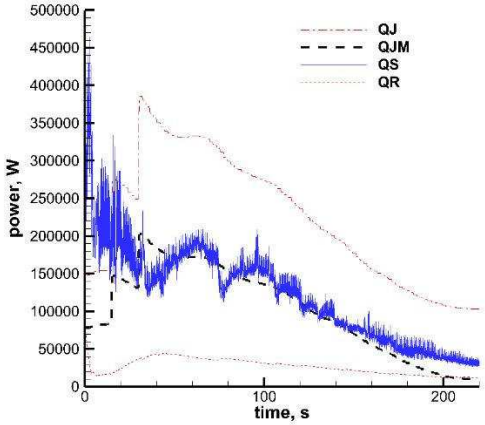

Figure 2. The time dependent variation of the induced electric heating and losses for the nozzle opening of 8 mm. QJ is the total Joule heating of the melt and the copper walls, QJM – melt only, QS – losses to the wall by the turbulent heat transfer, QR – radiation losses from the free surface.

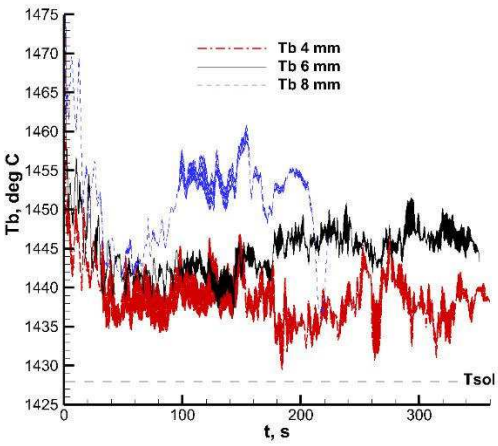

Figure 3. The liquid metal pouring temperature in C^{o} at the exit nozzle for the nozzle opening diameters 4, 6 and 8 mm.

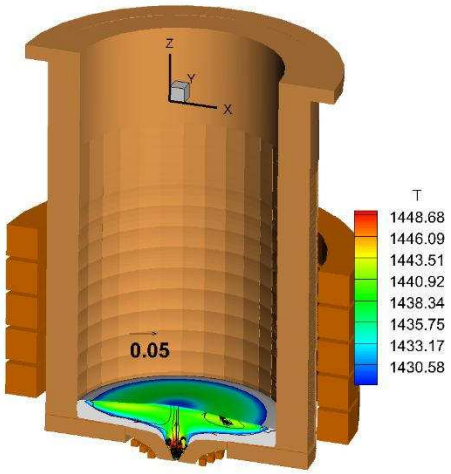

Figure 4. The cold crucible operation with the nozzle d = 4 mm at the final stage (870 s) just before the end of pouring when the nozzle freezes over.

CONCLUSIONS

The non-consumable nozzle consisting of liquid-cooled copper segments is presented to demonstrate beneficial features for titanium alloy melting in the cold crucible. The full cycle dynamic melting process is investigated using the time dependent numerical modelling.

REFERENCES

[1] Haun, R.E. (2017). Advances in the Systems and Processes for the Production of Gamma Titanium Aluminide Bars and Powder. *JOM*, 69, N 12, 2615-2620.

[2] Sillekens, W.H., et al. (2014). The ExoMet Project: EU/ESA Research on High-Performance Light-Metal Alloys and Nanocomposites. *Metall.Materials Trans*., 45A, 3349–3361.

[3] Tadano, H., Fujita, M., Take, T., Nagamatsu, K., Fukuzawa A. (1994). Levitational Melting of Several Kilograms of Metal with a Cold Crucible. *IEEE Trans. Magn*., 30(6), 4740-4742.

[4] Okumura, T., Shibata, T., Okochi, N. (2006). Production of Ti Alloy Gas Atomized Powder by Levitation Melting Furnace with Electric Nozzle. *Proc. 5th Internat. Conf. Electromagnetic Processing Materials*, Sendai, Japan, 784-789.

[5] Okumura, T., Yamamoto, K., Shibata, M. (2009). Large Scale Cold Crucible Levitation Melting Furnace with Bottom Tapping Nozzle. *Proc. 6th Internat. Conf. Electromagnetic Processing Materials*, Dresden, Germany, 521-524.

[6] Bojarevics, V., Harding, R.A., Pericleous, K. and Wickins M. (2004) The Development and Experimental Validation of a Numerical Model of an Induction Skull Melting Furnace *Metall. Materials Trans.*, 35B, 785-803.

[7] Bojarevics, V., Pericleous, K. (2018) Electromagnetic particle separation in the cold crucible melting with novel type bottom pouring nozzle. *Proc. 9th Internat. Conf. Electromagnetic Processing Materials*, IOP Conf. Series: Materials Science and Engineering, 424, 012029.

[8] Bojarevics, V., Pericleous, K. (2008) "Dynamic melting model for small samples in cold crucible", *COMPEL - The international journal for computation and mathematics in electrical and electronic engineering*, Vol. 27 Issue: 2, pp.350-358.

[9] Bojarevics, V., Roy, A. and Pericleous, K. (2011) "Numerical model of electrode induction melting for gas atomization", *COMPEL - The international journal for computation and mathematics in electrical and electronic engineering*, Vol. 30 Issue: 5, pp.1455-1466.